Journal of Alloys and Compounds 481 (2009) 87–90

Contents lists available at ScienceDirect

Journal of Alloys and Compounds

journal homepage: www.elsevier.com/locate/jallcom

Magnetic properties of B-rich (Fe, Co)–Nb–B amorphous alloys

I. Betancourt*, R. Landa

Departamento de Materiales Metalicos y Ceramicos, Instituto de Investigaciones en Materiales, Universidad Nacional Autonoma de Mexico, Mexico D.F. 04510, Mexico

ARTICLE INFO

Article history:
Received 26 February 2009
Received in revised form 23 March 2009
Accepted 25 March 2009
Available online 5 April 2009

PACS:
75.50.Kj
75.47.Np

Keywords:
Metallic glasses
Rapid solidification
Magnetization
Magnetostriction
Magnetic measurements

ABSTRACT

The magnetic properties of melt spun $Fe_{52-x}Co_{10+x}Nb_8B_{30}$ ($x = 0$, 12, 24, 36) amorphous ribbons are presented and discussed. The Curie temperature together with the saturation magnetization exhibited a progressive decrease with increasing Co addition (from 631 to 512 K and from 1.24 to 0.53 T, respectively). On the other hand, the ac initial magnetic permeability displayed a diminishing trend with increasing Co content, from 7500 to 1500 at $f = 0.5$ kHz together with a relaxation frequency variation between 2 and 7 kHz. In addition, the alloys magnetostriction showed a decreasing tendency with increasing cobalt concentration. Results are interpreted on the basis of the detrimental effect of Co on the intrinsic magnetic properties of the alloy series.

1. Introduction

Ferromagnetic amorphous Fe–Nb–B alloys with high B content (≥20 at%) are characterized by large supercooled liquid regions, with wide ΔT_x intervals in excess of 40 K ($\Delta T_x = T_x - T_g$, where T_x is the crystallization temperature and T_g the glass transition temperature) [1–3], which enables the possibility for obtaining bulk metallic glasses with critical diameters over 1 mm and excellent soft magnetic properties, e.g., large magnetic permeability at high frequencies, high saturation magnetization $\mu_0 M_s$ values and small magnetostriction constants [3,4]. For this kind of alloys, the effect of alloying addition (Zr, Y, W, Ta) and partial replacement of the transition metal constituent (Ni, Co, Ti) has been reported as having variable beneficial effects on the alloy glass forming ability, its thermal stability and on its magnetic and mechanical properties [4–6]. Nevertheless, no studies have been reported yet for the specific response of such amorphous alloys under ac applied fields, for which important magnetic aspects such as the magnetization reversal mechanism, the relaxation frequency and the magnetoelastic coupling can be determined. In this work, we present the effect of partial replacement of Fe by Co on the intrinsic and ac magnetic properties of B-enriched $Fe_{62}Nb_8B_{30}$ amorphous ribbons.

2. Materials and methods

The alloy ribbon series $Fe_{52-x}Co_{10+x}Nb_8B_{30}$ ($x = 0$, 12, 24, 36) was prepared by means of chill block melt spinning with a roll speed of 30 m/s, from initial ingots obtained from arc-melting of pure (99.99%) Fe, Co, Nb and B elements in a protective Ar atmosphere. The alloy ribbons microstructure was verified by means of XRD analysis with Cu-K_α radiation. The intrinsic magnetic properties were measured by Magnetic Thermogravimetric Analysis with an applied field of 0.1 T and by Vibrating Sample Magnetometry with a maximum field of 400 kA/m, for which the uncertainty was estimated from the standard deviation of at least 15 repetitions. The frequency dependent magnetic permeability was determined by means of an HP 4192A Impedance Analyzer coupled with a small solenoid producing a longitudinal h_{ac} field of 20 A/m within the frequency range 10 Hz–13 MHz.

3. Results and discussion

The fully amorphous structure across the compositional series was verified by XRD diffractograms, for which a distinctive single broad maximum was manifested (not included). Magnetic TGA curves for all the ribbon samples are shown in Fig. 1, for which the Curie temperature T_c exhibits a progressive decrease with increasing Co content, from 631 K for the initial $x = 0$ alloy ribbon to 512 K for $x = 36$. M–H loops for the whole alloy series are displayed in Fig. 2, showing a progressive decrease of $\mu_0 M_s$ values with Co addition, from 1.24 ± 0.16 T at the original $x = 0$, to 0.53 ± 0.05 T for the final $x = 36$. The alloy coercivities display minor variations between 0.90 ± 0.09 kA/m and 1.03 ± 0.15 kA/m. A summary of magnetic properties is listed in Table 1. This diminishing tendency for $\mu_0 M_s$ across the alloy series with decreasing Co concentration should be

* Corresponding author. Fax: +52 55 6161371.
E-mail address: israelb@correo.unam.mx (I. Betancourt).

0925-8388/$ – see front matter © 2009 Elsevier B.V. All rights reserved.
doi:10.1016/j.jallcom.2009.03.145

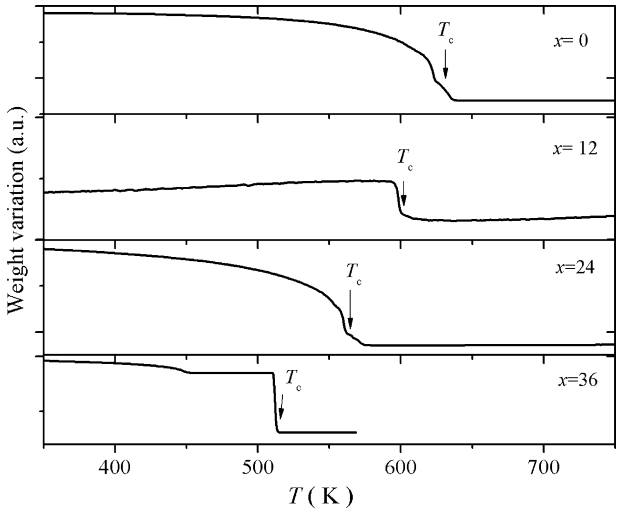

Fig. 1. Magnetic TGA curves for the $Fe_{52-x}Co_{10+x}Nb_8B_{30}$ alloy series.

ascribed to the lower magnetization saturation of cobalt (1.79 T), relative to iron (2.18 T). This reducing $\mu_0 M_s$ also determines the decreasing effect on the alloys ac permeability, as it is evidenced in Fig. 3a. The decreasing T_c is indicative of diminishing Fe–Fe, Fe–Co and Co–Co exchange interactions, for which similar reductions (of both T_c and $\mu_0 M_s$) with increasing Co additions have been reported for equivalent $Co_{1-x}Fe_xZrB$ [7], $Fe_{1-x}Co_xNbB$ [8,9] and $(Fe,Co)_{89}Zr_7B_4$ amorphous ribbons [10].

On the other hand, the real and imaginary components of the complex permeability $\mu^* = \mu_{re} + j\mu_{im}$ (with $j = \sqrt{-1}$) were determined from complex impedance $Z^* = Z_{re} + jZ_{im}$ measurements according to the relation [11,12]

$$\mu^* = G\left(\frac{-jZ^*}{\omega}\right) \quad (1)$$

where G is an appropriate geometrical factor and ω corresponds to the angular frequency. Both, real and imaginary components of permeability are shown in Fig. 3a and b, for which reduced values of μ_{re} are observed with increasing Co content, while μ_{im} exhibits also a diminishing tendency with increasing Co concentration. The spectroscopic μ_{re} (f) plots represent the initial permeability μ_i of the alloy, for which the magnetization mechanism is associated to the reversible bulging of magnetic domain walls, DWs [11,12]. Further increase in f causes a significant μ_{re} reduction, which is associated to a relaxation-type dispersion of the reversible bulging mechanism, for which the DWs are no longer able to follow the ac magnetic variations. Beyond the threshold frequency f_x (or relaxation frequency) μ_{re} becomes very small, reflecting the contribution of the spin rotation as the only magnetization process active at $f > f_x$ [11,12]. Complementary, the imaginary μ_{im} component is attributed to the alloy magnetic losses (hysteresis, eddy current, power losses) [11–13]. The maximum in μ_{im} corresponds to f_x. For the present alloy series, f_x exhibits an increasing tendency (Fig. 3b), which implies an improved alloy ability for sustaining magnetic initial permeability at increasing f values as consequence of a reduction of the magnetic losses, afforded for instance, by higher resistivity values.

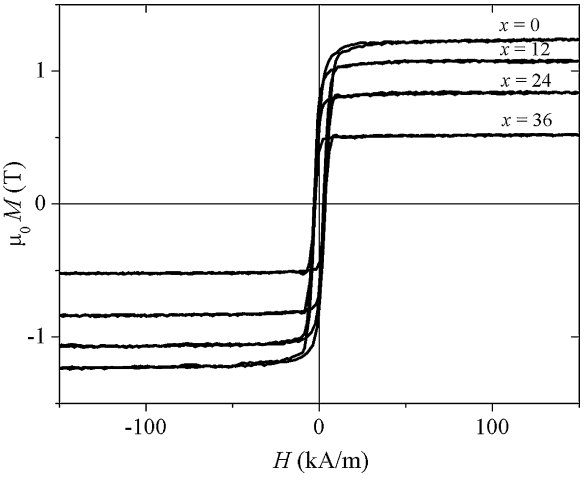

Fig. 2. Hysteresis M–H loops for the $Fe_{52-x}Co_{10+x}Nb_8B_{30}$ alloy series.

Table 1
Magnetic properties of the $Fe_{52-x}Co_{10+x}Nb_8B_{30}$ alloy series: Curie temperature, saturation magnetization, coercive field, relative initial permeability (at $f = 0.2$ kHz), relaxation frequency and saturation magnetostriction.

Co replacement x	T_c (K)	$\mu_0 M_s$ (T)	H_c (kA/m)	μ_i	f_x (kHz)	λ_s (10^{-6})
0	631 ± 2	1.24 ± 0.16	0.90 ± 0.09	7500	2	10.7
12	601 ± 3	1.09 ± 0.14	0.90 ± 0.14	7250	4	3.6
24	563 ± 3	0.86 ± 0.03	1.01 ± 0.16	1700	10	3.0
36	512 ± 2	0.53 ± 0.05	1.03 ± 0.15	1500	3	–

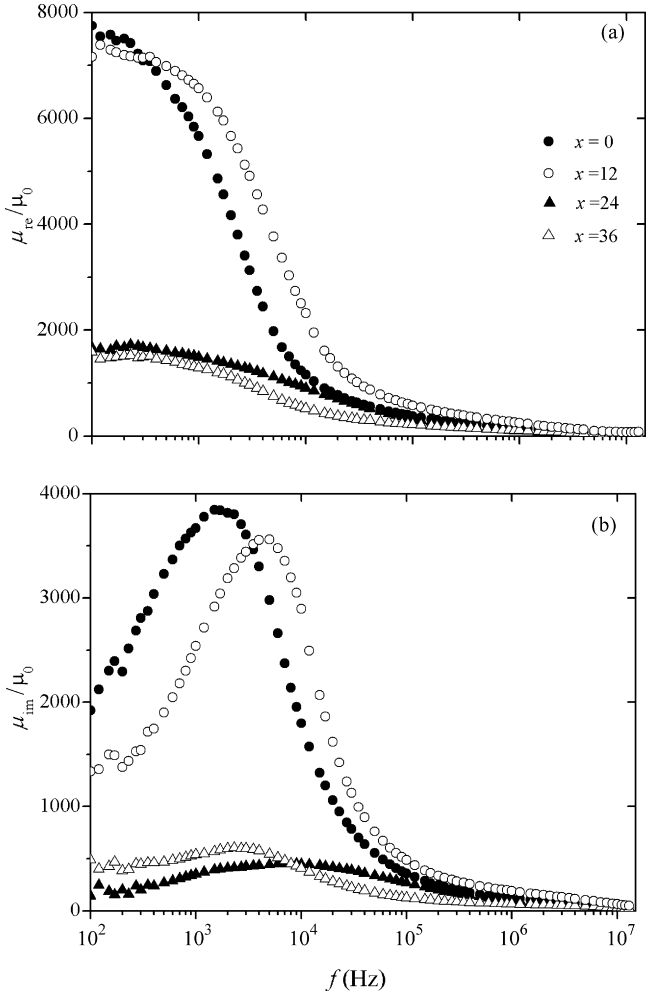

Fig. 3. Spectroscopic μ_{re} (f) (a) and $\mu_{im}(f)$ (b) plots for the $Fe_{52-x}Co_{10+x}Nb_8B_{30}$ alloy series.

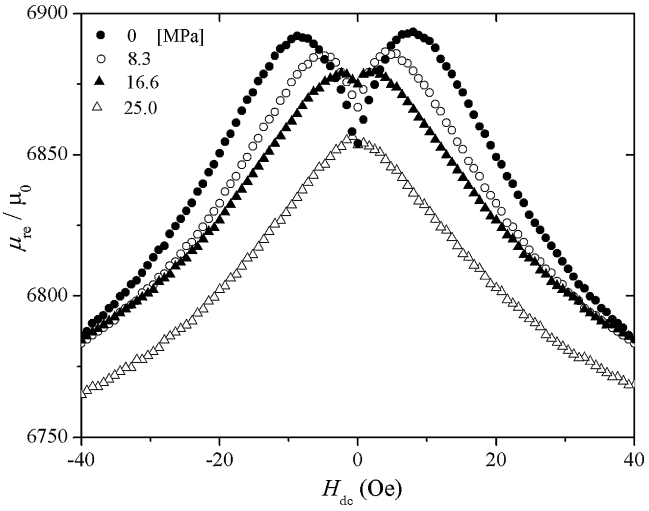

Fig. 4. $\mu_{re}(H_{dc})$ curves under the effect of variable tension stress σ for the $Fe_{52}Co_{10}Nb_8B_{30}$ alloy.

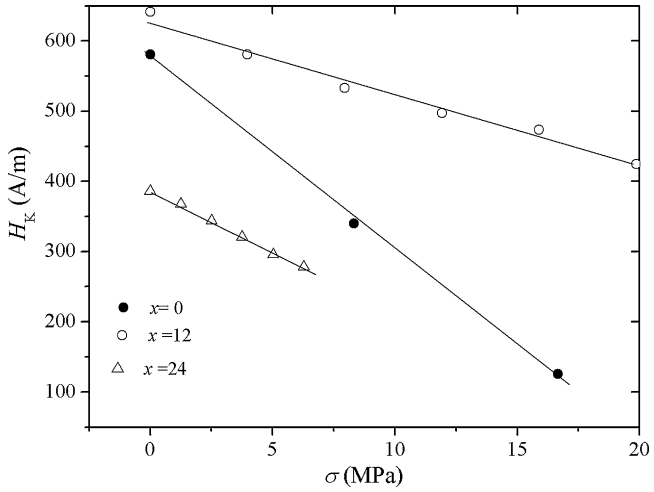

Fig. 5. Transverse anisotropy field H_k as a function of applied stress σ for the $Fe_{52-x}Co_{10+x}Nb_8B_{30}$ alloy series. The straight lines corresponds to linear fittings with at least $R^2 = 0.99$.

In order to monitor the magnetoelastic coupling across of the alloy series, μ_{re} plots as a function of applied dc field and under the effect of variable longitudinal applied tension stress σ at a constant frequency $f = 13$ MHz were determined for each composition. Fig. 4 illustrates μ_{re} (H_{dc})–σ curves for the $Fe_{52}Co_{10}Nb_8B_{30}$ alloy, for which at $\sigma = 0$, μ_{re} initially increases for H_{dc} values between 0 and 10 Oe, followed by a monotonous decrease for $H_{dc} > 10$ Oe. This behaviour is symmetrical for negative H_{dc}. For increasing σ, this original two-peak behaviour progressively evolves to a reduced single-maximum μ_{re} (H_{dc}) picture. Same tendencies were observed for the remaining alloy samples, except for the $x = 36$ alloy, which showed negligible magnetic permeability values as a consequence of its vanishing λ_s constant. The physical meaning of these μ_{re} (H_{dc})–σ plots can be explained as follows: At the frequency of measurement ($f = 13$ MHz $\gg f_x$), the spin rotation remains as the only active magnetization mechanism and thus, the real component of permeability corresponds to the rotational permeability μ_{re}^{rot}. For the stress-free curve, the initial increase of μ_{re}^{rot} up to $H_{dc} = 10$ Oe can be ascribed to an additional component (axially oriented) of μ_{re}^{rot} exerted by H_{dc}. The maximum in μ_{re}^{rot} is a consequence of a counterbalancing effect in the rotational magnetization process between the axial H_{dc} and the transverse anisotropy field H_k induced during the ribbon fabrication. Thus, the maximum in μ_{re}^{rot} (H_{dc}) corresponds to H_k [14,15]. For H_{dc} beyond 10 Oe, the rotational permeability decreases since the magnetic spins are mostly axially oriented after having overcome the original transverse anisotropy. On the other hand, for the μ_{re}^{rot} (H_{dc}) curves with increasing σ (up to 16.6 MPa), a shifting of H_k towards lower values is observed as a consequence of a progressively higher induced axial anisotropy, allowed by the increment of σ, which counterbalance the original transverse anisotropy and thus, the as-cast transverse magnetoelastic coupling. For $\sigma = 25.0$ MPa, the alloy transverse anisotropy is averaged out, which results in a single-peak regime with reduced μ_{re}^{rot} as a consequence of the predominant axial anisotropy induced by σ. This behaviour is indicative of a positive λ_s. The dependence of H_k on σ for alloy ribbons with $x \leq 36$ is displayed in Fig. 5, for which the following linear trends are manifested (after appropriate linear fittings): $H_k = 576\,[A/m] - 27.3 \times 10^{-6}\,[A/(mPa)]$ σ, $x = 0$; $H_k = 628\,[A/m] - 10.3 \times 10^{-6}\,[A/(mPa)]$ σ, $x = 12$; and $H_k = 387\,[A/m] - 17.7 \times 10^{-6}\,[A/(mPa)]$ σ, $x = 24$. From such functional relations is possible to estimate λ_s according to [15,16]:

$$\lambda_s = -\left(\frac{\mu_0 M_s}{3}\right)\left(\frac{\Delta H_z}{\Delta \sigma}\right) \quad (2)$$

where $\mu_0 M_s$ is the saturation magnetization and ΔH_z corresponds to the variations of the transverse field H_z necessary to compensate the magnetoelastic contribution induced by σ. This equation is proposed for both, positive and negative λ_s values [15,16]. For present measurements, the compensating ΔH_z field corresponds to H_k straightforward. Therefore, Eq. (2) becomes

$$\lambda_s = -\left(\frac{\mu_0 M_s}{3}\right)\left(\frac{H_k}{\Delta \sigma}\right) \quad (3)$$

Taking $\mu_0 = 12.56 \times 10^{-7}$ H/m and $\mu_0 M_s$ values from Table 1 and $H_k/\Delta\sigma$ as the slopes of the $H_k(\sigma)$ plots (Fig. 5), we found a decreasing λ_s tendency with increasing Co concentration (Table 1).

4. Conclusions

An overall detrimental effect on the magnetic properties of B-rich, Fe–Co–Nb–B amorphous alloys was found with increasing cobalt replacement for Fe. Optimum Co content for best soft magnetic properties correspond to the $Fe_{52}Co_{10}Nb_8B_{30}$ alloy, for which maximum saturation magnetization, Curie temperature and initial permeability values were observed.

Acknowledgements

I. Betancourt acknowledges the financial support from Research Grant IN106808 PAPIIT-UNAM, Mexico and also to Esteban Fregoso and Gabriel Lara for their valuable technical assistance.

References

[1] T. Itoi, A. Inoue, Mater. Trans. JIM 40 (1999) 643.
[2] T. Itoi, A. Inoue, Mater. Tans. JIM 41 (2000) 1256.
[3] M. Stoica, K. Hajlaoui, A. Lemoulec, A.R. Yavari, Philos. Mag. Lett. 86 (2006) 267.
[4] H. Chiriac, N. Lupu, Mater. Sci. Eng. A 375–377 (2004) 255.
[5] D.S. Song, J.-H. Kim, E. Fleury, W.T. Kim, D.H. Kim, J. Alloys Compd. 389 (2005) 159.
[6] J.M. Barandiaran, J. Bezanilla, H.A. Davies, P. Pawlik, Sens. Actuators A 129 (2006) 50.
[7] A. Inoue, H. Koshiba, T. Itoi, A. Makino, Appl. Phys. Lett. 73 (1998) 744.
[8] T. Itoi, A. Inoue, Appl. Phys. Lett. 74 (1999) 2510.
[9] T. Gloriant, S. Suriñach, M.D. Baró, J. Non-Cryst. Solids 333 (2004) 320.
[10] F. Johnson, C.Y. Um, M.E. McHenry, H. Garmestani, J. Magn. Magn. Mater. 297 (2006) 93.

[11] R. Valenzuela, J. Alloys Compd. 369 (2004) 40.
[12] R. Valenzuela, in: I. Betancourt (Ed.), Magnetic Materials: Current Topics in Amorphous Wires, Hard Magnetic Alloys, Ceramics, Characterization and Modelling, Research SignPost, Kerala, India, 2007, p. 1.
[13] S. Chikazumi, Physics of Magnetism, Robert E. Krieger Pub Co., New York, 1978, p. 327.
[14] L.V. Panina, K. Mohri, T. Uchiyama, M. Noda, IEEE Trans. Magn. 31 (1995) 1249.
[15] M. Knobel, M. Vazquez, L. Kraus, in: K.H.J. Buschow (Ed.), Giant Magneotimpedance, Handbook of Magnetic Materials, vol. 15, Elsevier North-Holland, Amsterdam, 2003, p. 497.
[16] A. Hernando, M. Vazquez, V. Madurga, J. Magn. Magn. Mater. 37 (1983) 161.